

# Efficiency Enhancement of Doherty Amplifier by Mitigating the Knee Voltage Effect

Junghwan Moon, *Student Member, IEEE*, Jangheon Kim, *Member, IEEE*, Jungjoon Kim, Ildu Kim, and Bumman Kim, *Fellow, IEEE*

**Abstract**—This paper presents an approach to mitigating the knee voltage effect of the Doherty power amplifier (PA), especially on the carrier amplifier. Such an effort increases the efficiency when the PA is driven by modulated signals. It is shown that, for the carrier PA,  $2R_{\text{opt}}$ , which is the theoretical value for the PA at a low power region, is not optimum condition when the knee voltage is not negligible. Due to the effect, the carrier PA is not in the saturated operation at the 6 dB back-off power level. To obtain the maximum efficiency at the region under the non-zero knee voltage, the load impedance of a carrier amplifier should be increased larger larger than that of conventional amplifier, i.e.,  $2R_{\text{opt}}$ , to reduce the knee voltage effect. By mitigating the effect, the optimized operation condition for efficiency is derived. The optimized Doherty amplifier is analyzed and simulated in terms of its load modulation behavior, efficiency, and output power, and compared with the conventional Doherty PA. The good performance is demonstrated by the Doherty PA built using Cree GaN HEMT CGH40045 devices at 2.655 GHz. For worldwide interoperability for microwave access applications with a 7.8 dB peak-to-average power ratio, the proposed PA delivers an efficiency of 49.3% at an output power of 42 dBm, which is a 7.5 dB back-off level from the peak power, with an acceptable linearity of  $-23.1$  dBc. The linearity is improved to  $-43$  dBc by employing a digital feedback predistortion technique, satisfying the system linearity specification.

**Index Terms**—Doherty, efficiency enhancement, gallium nitride, knee voltage, load modulation, power amplifier, worldwide interoperability for microwave access.

## I. INTRODUCTION

AS wireless communication systems utilize higher data rates, the signals of the systems vary rapidly and have large peak-to-average power ratios (PAPRs) because of the complex modulation schemes for efficient spectrum usage. To satisfy linearity requirements for the signals such as wideband code division multiple access, orthogonal frequency division multiple access, and world wide interoperability for microwave access (WiMAX), PAs should have a capability

of generating the peak power, and generate all power levels linearly following the signal distribution. Therefore, the PAs operate mostly at the average power level, back-off from the peak power by PAPR. The efficiency at the operation point is low, leading to a low efficiency PA. There are a few candidates that can solve the low efficiency problem due to the operation at a back-off power region, such as envelope elimination and restoration, envelope tracking, and Doherty PA [1]– [23]. The first two systems provide good efficiency by adjusting the drain/collector bias to reduce the dissipated power consumptions. However, they have some problems, such as difficulty of the delay adjustment of the RF and envelope paths and the complexity of the linkage between the PA and bias modulator. Moreover, they require a highly efficient bias modulator as well as the PA [4]– [7]. However, the Doherty PA can accomplish the high efficiency employing two PAs: one PA, carrier amplifier, is operational at a low power region, and another one, peaking amplifier, is turned on at a high power region. The power of the PAs are combined by the self-adjusted load modulation technique [8]– [23].

A significant amount of research has been focused on the Doherty PA to improve its efficiency. Asymmetrical Doherty PAs, such as an N-way Doherty PA [13], an extended Doherty PA [14], and a multistage Doherty PA [15] have been proposed to extend the peak efficiency region over a wider range of output power. In addition, the Doherty PA based on a saturated PA [16]– [19], such as the class-F and inverse class-F, shows the enhanced maximum efficiency. Although the previous works provide good theoretical analysis, they are performed in the ideal design environment. However, it is a challenging task to obtain the same high efficiencies at the peak and back-off power levels like an *Ideal Doherty*, as shown in Fig. 1. Thus, it is crucial to determine which region should be optimized for better overall-efficiency when the PA is driven by a modulated signal, and we have evaluated the efficiency of the Doherty PAs optimized at the each theoretical maximum region. *Doherty Type-I* shows a degraded efficiency at the peak power level, resulted from imperfect load modulation of the Doherty PA. *Doherty Type-II*, on the other hand, has reduced efficiency at the back-off power level because the carrier PA does not reach to the peak efficiency when the peaking PA is turned on. Based on these profiles, the estimated overall-efficiencies for amplification of the modulated signal with PAPR of 7.8 dB are computed using a routine coded in MATLAB and summarized in Table I [16]. Our results show that the Doherty amplifier's should be optimized for high efficiency at the back-off region and not at the peak power

Manuscript received September 3, 2009; revised February 10, 2010. This work was supported by the MKE (The Ministry of Knowledge Economy), Korea, under the ITRC (Information Technology Research Center) support program supervised by the NIPA (National IT Industry Promotion Agency)(NIPA-2010-(C1090-1011-0011)), by WCU (World Class University) program through the Korea Science and Engineering Foundation funded by the Ministry of Education, Science and Technology(Project No. R31-2008-000-10100-0), and by the Brain Korea 21 Project in 2010.

J. Moon, J. Kim, and B. Kim are with the Department of Electrical Engineering, Pohang University of Science and Technology, Pohang, Gyeongbuk 790-784, Korea (e-mail: jhmoon@postech.ac.kr; jungjoon@postech.ac.kr; bmkim@postech.ac.kr).

J. Kim and I. Kim are with the Samsung Electronics Company Ltd., Suwon, Gyeonggi, Korea (e-mail: jangheon.kim@samsung.com; ildul2.kim@samsung.com).

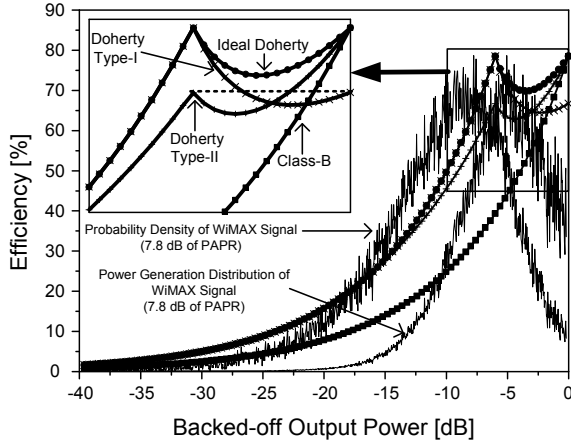


Fig. 1. Ideal efficiencies of the class-B and two-way Doherty power amplifiers and the probability density and power generation distribution of a WiMAX signal with a 7.8 dB PAPR.

TABLE I  
ESTIMATED EFFICIENCY OF TWO-WAY DOHERTY AMPLIFIERS FOR A SIGNAL WITH A PAPR OF 7.8 dB

	Ideal Doherty	Doherty Type I	Doherty Type II
$\eta_{avg}$ [%]	61.5	59.4	56.3

one to ensure better performance under modulated signals.

To get the maximum efficiency at the back-off region, the knee voltage effect of the carrier PA should be considered. We have found that a load impedance larger than  $2R_{opt}$  is needed in the low power region to obtain fully saturated operation when the peaking PA is turned on. Even though the basic design concept has been discussed previously [20], this study presents a more detailed analysis and further experimental results. We examine the basic operation of the Doherty PA in Section II. Section III describes the detailed behavior of the PA using real device simulation. To verify our analyses and simulations, we implement the amplifier using Cree GaN HEMT CGH40045 devices at 2.655 GHz and compared with the conventional Doherty PA for continuous wave (CW) and mobile WiMAX 1FA signals, which is explained in Section IV. The experimental results clearly show that the knee voltage effect should be considered to properly design the Doherty PA. Finally, the digital feedback predistortion (DFBPD) technique is applied to achieve highly linear performance [24], satisfying the system specifications.

## II. ANALYSIS FOR OPERATIONAL CHARACTERISTICS OF THE DOHERTY POWER AMPLIFIER

### A. Doherty PA Operation with Knee Voltage Effect

Theoretically, the Doherty PA attains the highest efficiencies at the 6 dB back-off and at the peak power levels. The maximum efficiencies at the two points can be achieved with perfect load-modulated-operation of the carrier and peaking PAs and infinite output impedance of the peaking PA at the turn-off state. The perfect load modulation of the carrier PA with zero-knee voltage, depicted in Fig. 2(a), indicates that

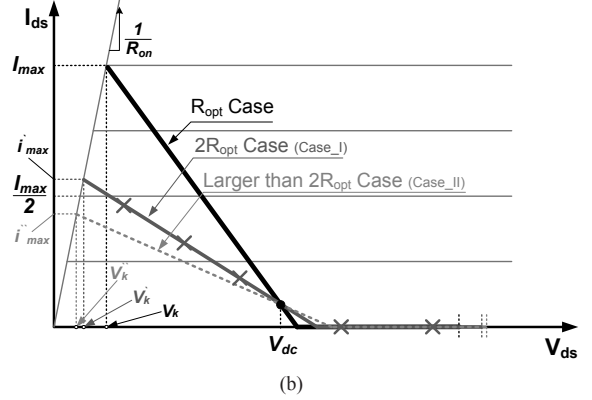
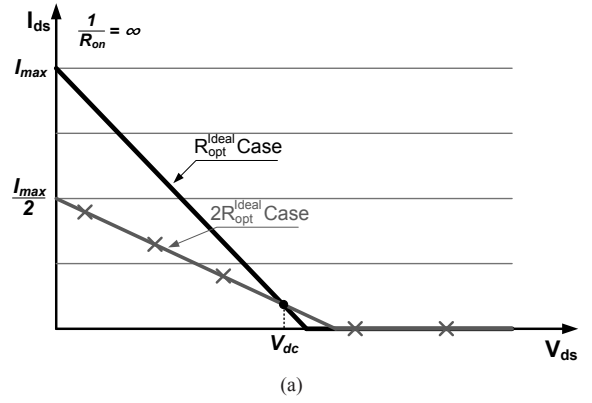


Fig. 2. Load line of the carrier amplifier. (a) Ideal case with zero knee voltage. (b) Practical case with non-zero knee voltage.

the output powers for both  $R_{opt}^{Ideal}$  and  $2R_{opt}^{Ideal}$  are  $P_1^{Ideal}$  and  $P_1^{Ideal}/2$ , respectively. The efficiencies ( $\eta^{Ideal}$ s) are also the same at  $P_1^{Ideal}$  and  $P_1^{Ideal}/2$ , respectively; the carrier PA is in equally saturated states for both cases. In this operation,  $P_1^{Ideal}$ ,  $\eta^{Ideal}$ , and  $R_{opt}^{Ideal}$  are given by

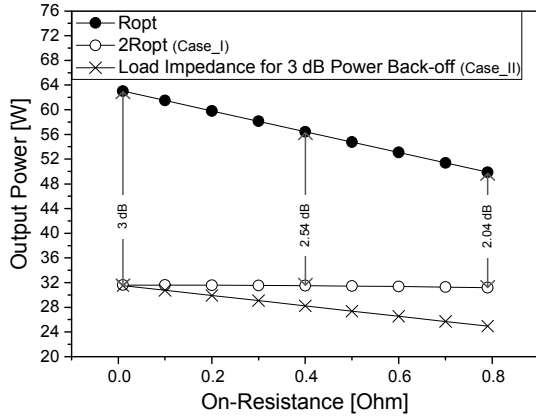
$$\begin{aligned}
 P_1^{Ideal} &= \frac{1}{2} \cdot I_{1,c}(\theta_c) \cdot V_1 \\
 \eta^{Ideal} &= \frac{P_1^{Ideal}}{P_{dc}^{Ideal}} \times 100 = \frac{(1/2) \cdot I_{1,c}(\theta_c)}{I_{dc,c}(\theta_c)} \times 100 \\
 R_{opt}^{Ideal} &= \frac{V_1}{I_{1,c}(\theta_c)}
 \end{aligned} \tag{1}$$

where

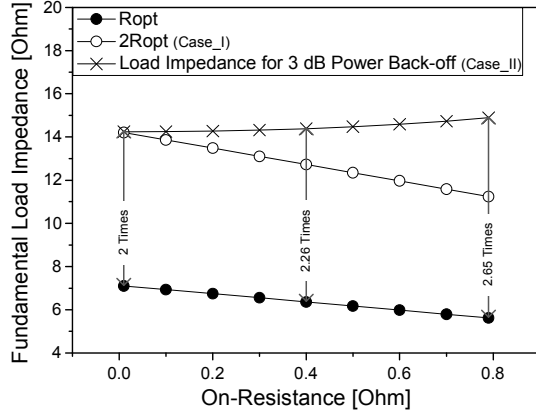
$$\begin{aligned}
 I_{1,c}(\theta_c) &= \frac{I_{max}}{2\pi} \cdot \frac{\theta_c - \sin \theta_c}{1 - \cos(\theta_c/2)} \\
 I_{dc,c}(\theta_c) &= \frac{I_{max}}{2\pi} \cdot \frac{2 \cdot \sin(\theta_c/2) - \theta_c \cdot \cos(\theta_c/2)}{1 - \cos(\theta_c/2)}.
 \end{aligned}$$

$I_{1,c}(\theta_c)$  and  $I_{dc,c}(\theta_c)$  are the fundamental and dc current components of the carrier PA biased at the conduction angle  $\theta_c$ , respectively. In the ideal case,  $V_1$  is equal to  $V_{dc}$  because of the zero on-resistance  $R_{on}$  with the zero knee voltage.

In a real device, the effect of knee voltage should be considered. Fig. 2(b) shows a load line with the knee voltage



(a)



(b)

Fig. 3. (a) Maximum output powers employing  $R_{\text{opt}}$ ,  $R^{\text{Case}_I}$ , and  $R^{\text{Case}_{II}}$  as  $R_{\text{on}}$  varies from 0 to 0.8  $\Omega$ . (b) Load impedances for  $R_{\text{opt}}$ ,  $R^{\text{Case}_I}$ , and  $R^{\text{Case}_{II}}$  as  $R_{\text{on}}$  varies from 0 to 0.8  $\Omega$ .

$V_k$ . For  $R_{\text{opt}}$  and  $2R_{\text{opt}}$ , the load impedances are written by

$$R_{\text{opt}} = \frac{V_{\text{dc}} - V_k}{I_{1,c}(\theta_c)} \quad (2)$$

$$R^{\text{Case}_I} = \frac{V_{\text{dc}} - V'_k}{i'_{1,c}(\theta_c)} \quad (3)$$

where

$$i'_{1,c}(\theta_c) = \frac{i'_{\text{max}}}{2\pi} \cdot \frac{\theta_c - \sin \theta_c}{1 - \cos(\theta_c/2)}$$

$$V_k = R_{\text{on}} \cdot I_{\text{max}}$$

$$V'_k = R_{\text{on}} \cdot i'_{\text{max}}$$

Since  $\text{Case}_I$  represents the  $2R_{\text{opt}}$  case,  $i'_{\text{max}}$  can be derived using (2) and (3) as follows:

$$i'_{\text{max}} = \frac{I_{\text{max}} V_{\text{dc}}}{2V_{\text{dc}} - I_{\text{max}} R_{\text{on}}} \quad (4)$$

$i'_{\text{max}}$  represents the maximum current when the carrier PA has a load impedance of  $2R_{\text{opt}}$ . Thus, the output powers for the

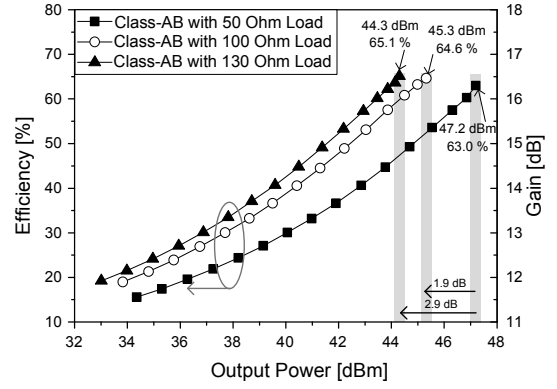


Fig. 4. Load modulation results for carrier amplifier employing the load impedances of 50  $\Omega$ , 100  $\Omega$ , and 130  $\Omega$ .

$R_{\text{opt}}$  and  $R^{\text{Case}_I}$  cases can be calculated as follows

$$P_{R_{\text{opt}}} = \left(\frac{1}{2}\right) \cdot I_{1,c}(\theta_c) \cdot (V_{\text{dc}} - V_k)$$

$$P^{\text{Case}_I} = \left(\frac{1}{2}\right) \cdot i'_{1,c}(\theta_c) \cdot (V_{\text{dc}} - V'_k) \quad (5)$$

and are shown in Fig. 3(a). For the calculation, we assume a  $V_{\text{dc}}$  supply of 30 V and  $I_{\text{max}}$  of 8 A with uniform transconductance.  $\theta_c$  is fixed at  $210^\circ$ . As shown, the carrier PA with  $2R_{\text{opt}}$  delivers more power than the expected value of  $(1/2)P_{R_{\text{opt}}}$  because of the enlarged voltage and current swings from  $(V_{\text{dc}} - V_k)$  to  $(V_{\text{dc}} - V'_k)$  and from  $I_{\text{max}}/2$  to  $i'_{\text{max}}$ , respectively. The efficiency deteriorates in the 6 dB back-off region of the Doherty PA because the carrier PA does not reach to the saturation state when the peaking PA begins conducting.

To maximize the efficiency at the 6 dB back-off power region, the carrier PA with non-zero knee voltage should have a load impedance larger than  $2R_{\text{opt}}$ , like the case-II in Fig. 2(b), because the carrier PA with  $2R_{\text{opt}}$  cannot be fully saturated at the 3 dB back-off region, as depicted in Fig. 3(a). In this case, the output power can be written as

$$P^{\text{Case}_{II}} = \left(\frac{1}{2}\right) \cdot i''_{1,c}(\theta_c) \cdot (V_{\text{dc}} - V''_k) \quad (6)$$

where

$$i''_{1,c}(\theta_c) = \frac{i''_{\text{max}}}{2\pi} \cdot \frac{\theta_c - \sin \theta_c}{1 - \cos(\theta_c/2)}$$

$$V''_k = R_{\text{on}} \cdot i''_{\text{max}}$$

Since  $P^{\text{Case}_{II}}$  should be a half of  $P_{R_{\text{opt}}}$  to obtain the fully saturated state at the 3 dB back-off region,  $i''_{\text{max}}$ , the maximum current when the carrier PA has a load impedance larger than  $2R_{\text{opt}}$ , can be calculated as follows

$$i''_{\text{max}} = \frac{1}{R_{\text{on}}} \cdot \frac{V_{\text{dc}} - \sqrt{(V_{\text{dc}})^2 - 2 \cdot V_k \cdot (V_{\text{dc}} - V_k)}}{2} \quad (7)$$

Fig. 3(b) shows the required load impedance with varying  $R_{\text{on}}$ . As  $R_{\text{on}}$  increases, the load impedance of the carrier PA in a low power region also increases larger than  $2R_{\text{opt}}$ , leading to the fully saturated state of the PA at the 6 dB back-off level.

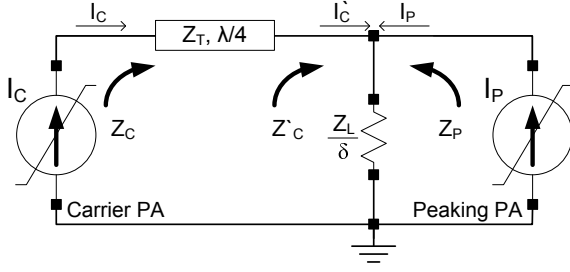


Fig. 5. Operational diagram of the proposed Doherty amplifier.

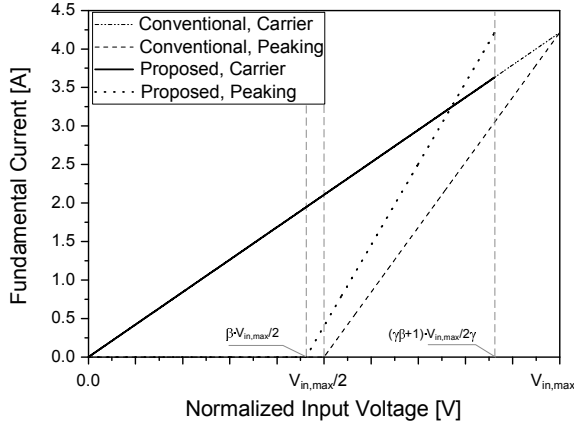


Fig. 6. Fundamental currents of the conventional and proposed Doherty PA according to the input voltage ( $\theta_c = 210^\circ$  and  $\theta_p = 150^\circ$ ).

To verify the knee voltage effects on the Doherty operation, especially the carrier PA, we implement the carrier PA using a Cree GaN HEMT CGH40045 device with a 45-W peak envelope power at 2.655 GHz. First, the output of the PA is matched to  $R_{opt}$  from  $50 \Omega$ . Then, its load impedance is modulated by adjusting the offset line and output termination impedance [11]. Fig. 4 shows the load modulation results for the carrier PA employing the output termination impedances of  $50 \Omega$ ,  $100 \Omega$ , and  $130 \Omega$ . As expected, the PA with  $100 \Omega$  delivers maximum efficiency at 45.3 dBm, which is 1.9 dB back-off power from the maximum output power of 47.2 dBm with the output termination impedance of  $50 \Omega$ . On the other hand, the PA with  $130 \Omega$  has its maximum efficiency at the 2.9 dB back-off point. Initially, the load impedance for the maximum efficiency at the 3 dB back-off level is determined by  $i''_{max}$ ,  $i''_{1,c}(\theta_c)$ , and  $V''_k$ , and then further optimized to achieve maximum efficiency at the 3 dB back-off power level.

### B. Load Modulation Behavior of Doherty Amplifier with Optimized Carrier PA

The fundamental operating principle and efficiency analysis of the Doherty amplifier have been well described in [8]–[23]. To design the Doherty amplifier properly for the real device, we suggest that the knee voltage effect should be considered, as described in Section II-A. Fig. 5 shows an operational diagram of the proposed Doherty PA used to analyze load modulation behavior, efficiency, and output power. Compared

to the conventional Doherty PA, it has a scaled load impedance of  $Z_L/\delta$  at the output power combining point.

For simplicity, it is assumed that each current source is linearly proportional to the input voltage signal with the maximum current of  $I_{max}$ . The ideal harmonic short circuits are provided so that the output power and efficiency can be determined using only the fundamental and dc components. The load impedances of the carrier and peaking amplifiers are determined by the current ratios of each amplifier. Since the load impedance of the carrier PA is larger than that of the conventional PA for the power levels, the current of the carrier amplifier cannot reach to the maximum value. However, for the peaking PA, it is assumed to reach the same maximum output current values for the conventional and proposed amplifiers. Thus, the load cannot be properly modulated in this structure, which is a disadvantage, leading to the degradation of output power. The peaking PAs of the conventional and proposed Doherty PAs start conducting when the carrier amplifiers generate the half of those maximum output power. In addition, the peaking PA is unevenly driven for proper load modulation [12], [17].

The fundamental currents of the conventional and proposed Doherty PAs based on the input voltage are represented in Fig. 6 and given by

$$I_C = \frac{I_{1,c}(\theta_c)}{V_{in,max}} \cdot v_{in}, \quad 0 \leq v_{in} \leq \frac{\gamma\beta + 1}{2\gamma} \cdot V_{in,max} \quad (8)$$

$$I_{DC,C} = \frac{I_{dc,c}(\theta_c)}{V_{in,max}} \cdot v_{in}, \quad 0 \leq v_{in} \leq \frac{\gamma\beta + 1}{2\gamma} \cdot V_{in,max} \quad (9)$$

$$I_P = \begin{cases} 0, & 0 \leq v_{in} < (\beta/2) V_{in,max} \\ \gamma \cdot \sigma \cdot I_{1,p}(\theta_p) \cdot \left( \frac{v_{in}}{V_{in,max}} - \frac{\beta}{2} \right), & (\beta/2) V_{in,max} \leq v_{in} \leq (\gamma\beta + 1) V_{in,max}/2\gamma \end{cases} \quad (10)$$

$$I_{DC,P} = \begin{cases} 0, & 0 \leq v_{in} < \beta \cdot V_{in,max}/2 \\ \gamma \cdot \sigma \cdot I_{dc,p}(\theta_p) \cdot \left( \frac{v_{in}}{V_{in,max}} - \frac{\beta}{2} \right), & (\beta/2) V_{in,max} \leq v_{in} \leq (\gamma\beta + 1) V_{in,max}/2\gamma \end{cases} \quad (11)$$

where

$$\begin{aligned} I_{1,p}(\theta_p) &= \frac{I_{max}}{2\pi} \cdot \frac{\theta_p - \sin \theta_p}{1 - \cos(\theta_p/2)} \\ I_{dc,p}(\theta_p) &= \frac{I_{max}}{2\pi} \cdot \frac{2 \cdot \sin(\theta_p/2) - \theta_p \cdot \cos(\theta_p/2)}{1 - \cos(\theta_p/2)} \\ \beta &= \frac{2 \cdot i''_{max}}{I_{max}} \\ &= \frac{V_{dc} - \sqrt{(V_{dc})^2 - 2 \cdot V_k \cdot (V_{dc} - V_k)}}{V_k} \\ \sigma &= \frac{2 \cdot I_{1,c}(\theta_c)}{I_{1,p}(\theta_p)}. \end{aligned}$$

$I_C$ ,  $I_P$ ,  $I_{DC,C}$ , and  $I_{DC,P}$  denote the fundamental and dc current components of the carrier and peaking PAs, respectively. As explained in Section II-A, the load impedance of the carrier amplifier in the proposed Doherty PA has larger load impedance than  $2R_{opt}$ , leading to an increment on the voltage swing in comparison with the conventional carrier amplifier,

as shown in Fig. 2(b). In order to deliver the same output power for both conventional and proposed PAs at the 6 dB back-off level, a current reduction is required. Compared to the conventional Doherty amplifier, a current of the carrier amplifier in the proposed Doherty amplifier is reduced by  $\beta$ .  $\sigma$  indicates the uneven power drive ratio [12].

By using the currents of the carrier and peaking PAs, the load impedances of the two PAs are given by

$$Z_C = \begin{cases} \frac{\delta \cdot Z_T^2}{Z_L \delta \cdot Z_T^2}, & 0 \leq v_{in} < \frac{\beta}{2} \cdot V_{in,max} \\ Z_L \cdot \left[ 1 + \frac{I_P}{I_C'} \right], & \frac{\beta}{2} \cdot V_{in,max} \leq v_{in} \leq \frac{\gamma\beta + 1}{2\gamma} \cdot V_{in,max} \end{cases} \quad (12)$$

$$Z_P = \begin{cases} \infty, & 0 \leq v_{in} < \frac{\beta}{2} \cdot V_{in,max} \\ \frac{Z_L}{\delta} \cdot \left( 1 + \frac{I_C'}{I_P} \right), & \frac{\beta}{2} \cdot V_{in,max} \leq v_{in} \leq \frac{\gamma\beta + 1}{2\gamma} \cdot V_{in,max} \end{cases} \quad (13)$$

where

$$\delta = \frac{R^{Case\_II}}{R^{Case\_I}} = \frac{V_{dc} + \sqrt{(V_{dc})^2 - 2 \cdot V_k \cdot (V_{dc} - V_k)}}{2 \cdot \beta \cdot (V_{dc} - V_k)}.$$

By assumption of a lossless quarter-wave transmission line in Fig. 5,  $I_C'$  is defined by

$$I_C' = \delta \cdot I_C \cdot \frac{Z_T}{Z_L} - I_P.$$

Since the carrier PA of the proposed Doherty amplifier has larger load impedance than conventional PA, the carrier amplifier operates in the hardly saturated region after the peaking amplifier is turned on. To prevent the clips of the voltage and current for the carrier amplifier, an additional uneven power drive of the peaking amplifier is required, lowering the load impedance of the carrier amplifier.  $\gamma$  represents the additional uneven power drive ratio. For the linear operation of the carrier PA, the voltage across the current source of the carrier cell should satisfy following condition at the maximum input voltage:

$$Z_C \cdot I_C \leq V_{dc} - \frac{\gamma\beta + 1}{2\gamma} \cdot V_k. \quad (14)$$

From (14),  $\gamma$  can be inferred and is given by

$$\gamma \geq \frac{2\delta R_{opt} I_{1,c}(\theta_c) + V_k}{2V_{dc} - 2R_{opt} I_{1,c}(\theta_c)(\beta\delta - 1) - \beta V_k}. \quad (15)$$

In this analysis, we use  $Z_T=R_{opt}$  and  $Z_L=R_{opt}/2$ .  $\delta$  signifies the necessary ratio of  $R^{Case\_I}$  to  $R^{Case\_II}$  to achieve the fully saturated operation of the carrier PA at the back-off region. For the conventional case,  $\delta$ ,  $\gamma$ , and  $\beta$  are equal to one. Thus, the fundamental load impedance of the carrier PA is modulated from  $2R_{opt}$  to  $R_{opt}$ , and that of the peaking PA varies from  $\infty$  to  $R_{opt}$ . On the other hand, for the proposed Doherty PA,  $\delta$  and  $\gamma$  are greater than

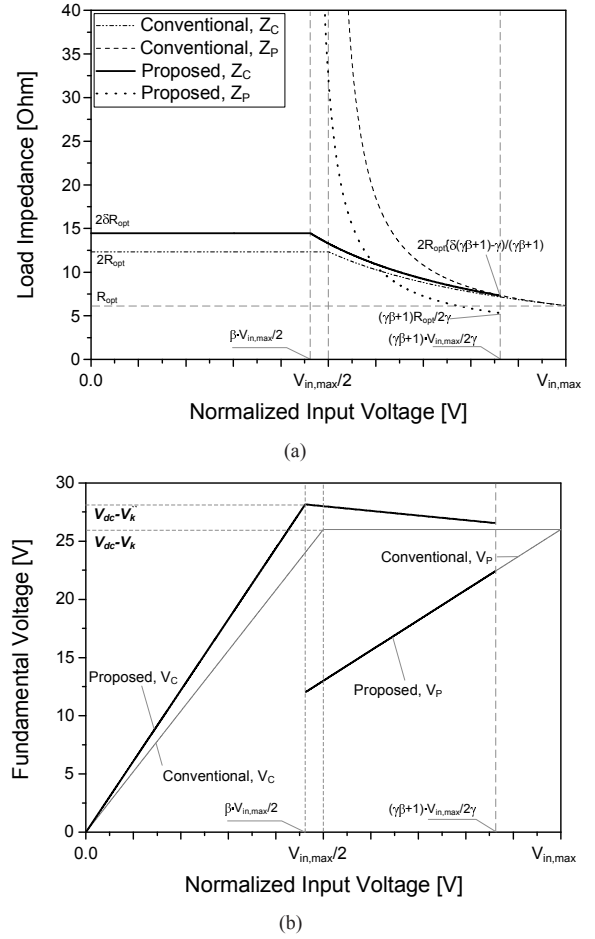


Fig. 7. (a) Load impedances of the conventional and proposed Doherty PA according to the input voltage. (b) Fundamental voltages of the carrier ( $V_C$ ) and peaking ( $V_P$ ) amplifiers for the conventional and proposed Doherty PAs.

one, but  $\beta$  is less than one. Thus, the fundamental load impedances of the carrier and peaking PAs are modulated from  $2\delta R_{opt}$  to  $2R_{opt} \{ \delta (\gamma\beta + 1) - \gamma \} / (\gamma\beta + 1)$  and from  $\infty$  to  $R_{opt} (\gamma\beta + 1) / 2\gamma$ , as described in Fig. 7(a). To explore the load modulation behavior,  $V_k$  of 4 V is assumed and  $R_{opt}$  is calculated by (2). At the low power region ( $0 \leq v_{in} < \beta V_{in,max}/2$ ), the load impedance for the carrier PA is larger than  $2R_{opt}$ , i.e.,  $2\delta R_{opt}$ . Moreover, at the high power region ( $\beta V_{in,max}/2 \leq v_{in} \leq (\gamma\beta + 1) V_{in,max}/2\gamma$ ), the load impedance of the carrier PA maintains a value larger than conventional PA. In contrast, the load impedance of the peaking PA sustains a smaller value than that of the conventional PA, which results in a slight power degradation. Fig. 7(b) shows the resulting fundamental voltages of the carrier and peaking amplifiers for the conventional and proposed Doherty PAs. As expected, compared with the conventional PA, at the low power region, the carrier amplifier for the proposed amplifier has the larger fundamental voltage due to the larger load impedance. It leads to the carrier PA can be fully saturated state, delivering the better efficiency.

By using the currents and load impedances of the carrier and peaking PAs, the efficiency can be estimated. Fig. 8

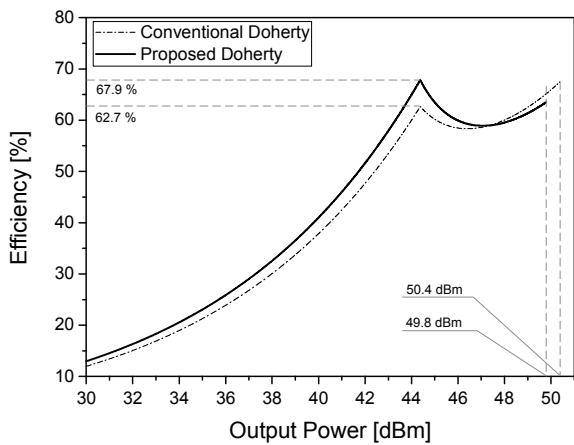


Fig. 8. Efficiencies of the conventional and proposed Doherty PA according to the output power.

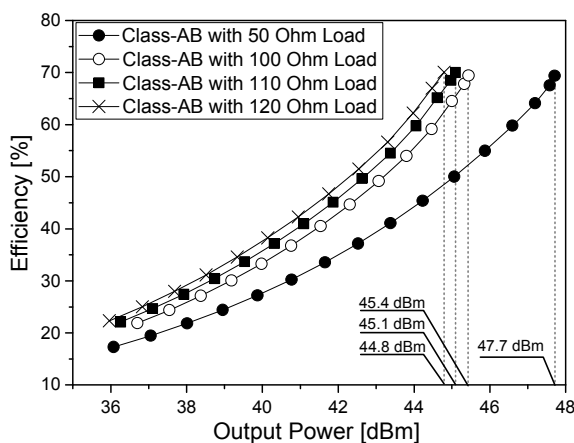


Fig. 9. Simulated load modulation results for the carrier PA with the load impedances of 50  $\Omega$ , 100  $\Omega$ , 110  $\Omega$ , and 120  $\Omega$ .

represents the calculated efficiencies based on the above analysis for  $\theta_c=210^\circ$  and  $\theta_p=150^\circ$  using MATLAB. To calculate the efficiencies,  $\delta$ ,  $\beta$ ,  $\sigma$ , and  $\gamma$  are determined by  $V_{dc}$ ,  $V_k$ ,  $I_{1,c}(\theta_c)$ , and  $I_{1,p}(\theta_p)$ , which are 30 V, 4 V, 4.2129 A, and 3.6384 A, respectively. The resulting  $\delta$ ,  $\beta$ ,  $\sigma$ , and  $\gamma$  are 1.1725 and 0.9235, 2.3158, and 1.2494, respectively. In the low power region, the proposed Doherty PA has higher efficiency than that of the conventional PA because of its larger load impedance. In particular, the proposed Doherty PA delivers its maximum efficiency of 67.9% at the 6 dB back-off output power, which is an increase of about 5% compared with the conventional one. Although the maximum output power and efficiency at the maximum output power are slightly degraded because of the imperfect load modulation characteristic, the proposed Doherty scheme improves efficiency for modulated signals without any additional circuitry.

### III. SIMULATION RESULTS

In Section II, we proposed a Doherty PA design considering the knee voltage effect, and analyzed efficiency and output power of the PA. To verify the analysis and investigate the

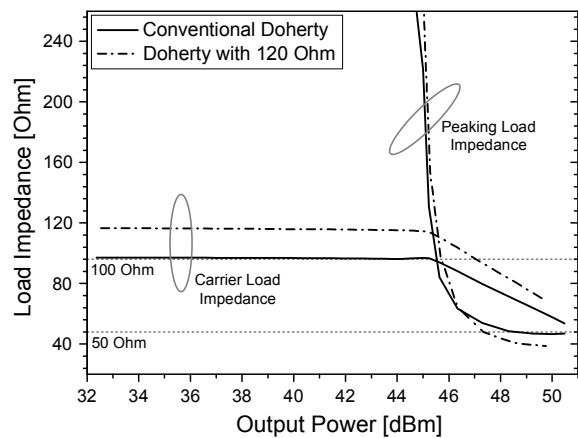


Fig. 10. Simulated load impedances of the conventional and proposed Doherty PAs as a function of the output power.

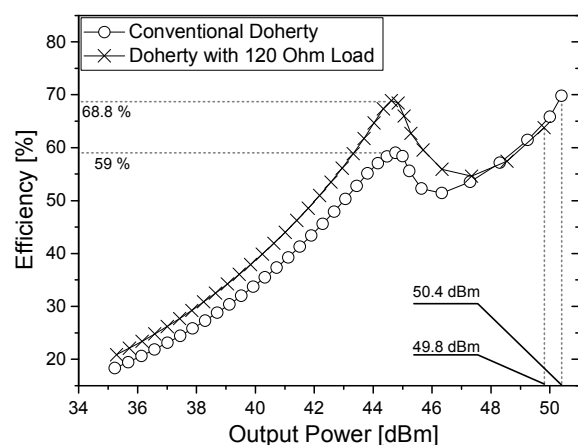


Fig. 11. Simulated efficiencies of the conventional and proposed Doherty PAs according to the output power.

real behavior of the PA, we performed ADS simulation using Cree's large signal model for CGH40045 GaN HEMT. The unit cell PA was designed to deliver maximum efficiency while maintaining the maximum output power. The quiescent current of the carrier cell was set to 200 mA, and the gate voltage of the peaking cell was adjusted to turn on at the 6 dB back-off power level.

To find the load impedance of the carrier PA delivering the maximum efficiency at the 3 dB back-off from peak output power, we simulated load modulation test. Fig. 9 illustrates the simulated efficiencies for a carrier PA with the output termination impedances of 50  $\Omega$ , 100  $\Omega$ , 110  $\Omega$ , and 120  $\Omega$ . As expected, the carrier PA with 100  $\Omega$  delivers its maximum efficiency at an output power of 45.1 dBm, which is 2.6 dB back-off power from the maximum output power of 47.7 dBm with the output termination impedance of 50  $\Omega$ . For the PA with 120  $\Omega$ , its maximum efficiency is achieved at the 2.9 dB back-off power level. As a result, we selected 120  $\Omega$  for the carrier PA at the low power region, i.e., before the peaking PA starts to turn on. Compared to the analytical value obtained from Fig. 3, we conclude that the output termination

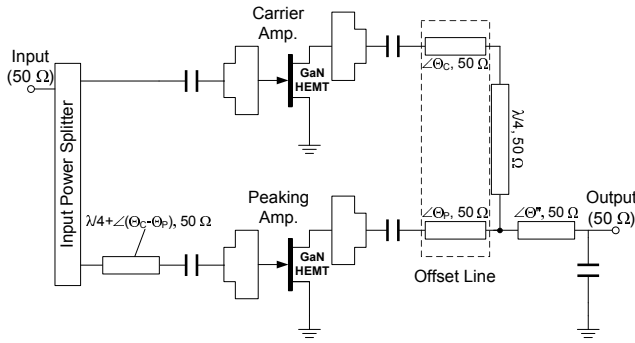


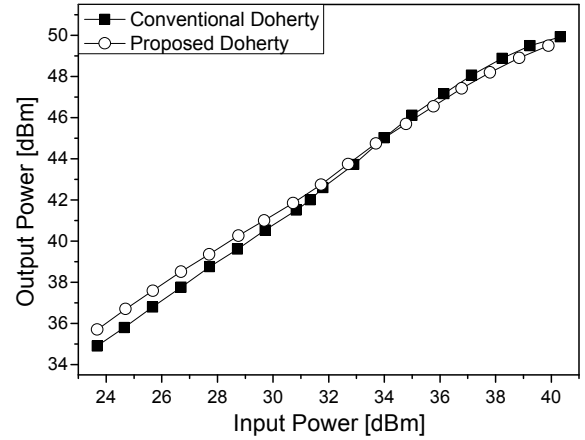
Fig. 12. Schematic diagram of the proposed Doherty PA.

impedance of  $120 \Omega$  is reasonable.

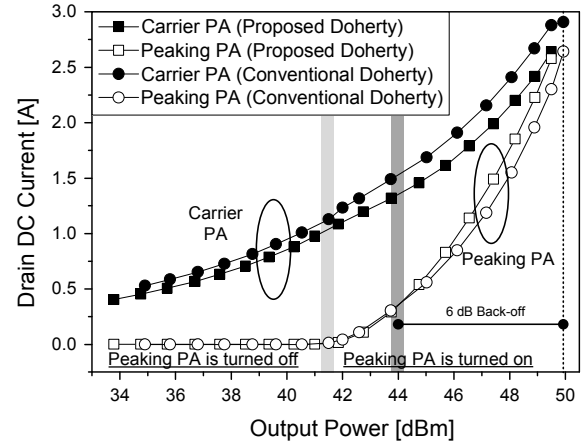
Fig. 10 shows the simulated load impedances of the conventional and proposed Doherty PA according to the output power. For the conventional case, the load impedance of the carrier PA modulates  $\sim 100 \Omega$  to  $\sim 50 \Omega$ , and that of the peaking PA also modulates  $\infty$  to  $\sim 50 \Omega$ . On the other hand, for the proposed case, the load impedance of the carrier PA remains  $120 \Omega$  until the peaking PA turn on. At the high power region, the load impedance of the carrier PA remains higher than  $50 \Omega$ , and that of the peaking PA is lower than  $50 \Omega$ . These results agree with the analysis given in Section II-B. Fig. 11 represents the simulated efficiencies of the conventional and proposed Doherty PAs according to the output power. Because of the larger load impedance at the low power region, the proposed Doherty PA improves the efficiency. In particular, the proposed PA delivers 68.8% of maximum efficiency at the low power region, which is an improvement of about 10% compared to that of the conventional PA. However, at the high power region, the output power and efficiency of the proposed Doherty PA are slightly degraded because of the inevitable imperfection of load modulation. However, the proposed Doherty PA delivers the desired efficiency for the modulated signal.

#### IV. IMPLEMENTATIONS AND MEASUREMENT RESULTS

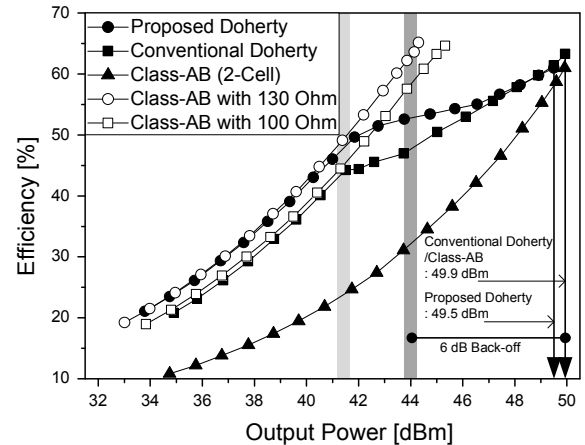
In Section II-A, we have shown that, for the Doherty PA, the carrier amplifier should have a load impedance larger than  $100 \Omega$  to improve the efficiency at the back-off region before the peaking PA turns on. This result is verified using ADS simulation, as explained in Section III. To experimentally validate the proposed Doherty scheme, a 2.655 GHz Doherty PA was fabricated using two Cree CGH40045 GaN HEMTs. For good efficiency, the two unit cell PAs are optimized for efficiency with reasonable output power [16], [17]. Fig. 12 shows schematic diagram of the proposed Doherty PA. In contrast with the conventional Doherty scheme, its output combiner consists of a  $50 \Omega$  transmission line  $\theta'$  and a parallel connected capacitor to easily change the output load impedance. In the experiment, the offset lines of the carrier PAs  $\theta_c$  are optimized to deliver maximum performance with  $100 \Omega$  and  $130 \Omega$ . The offset lines of the peaking PAs  $\theta_p$  are also adjusted to block the output power leakage from the carrier to the peaking PA; the transformed output impedance is  $1200 \Omega$ .



(a)



(b)



(c)

Fig. 13. Measured performances of the conventional and proposed Doherty amplifiers for a CW signal: (a) Output power versus input power. (b) Drain dc supply current as a function of the output power. (c) Drain efficiency according to the output power.

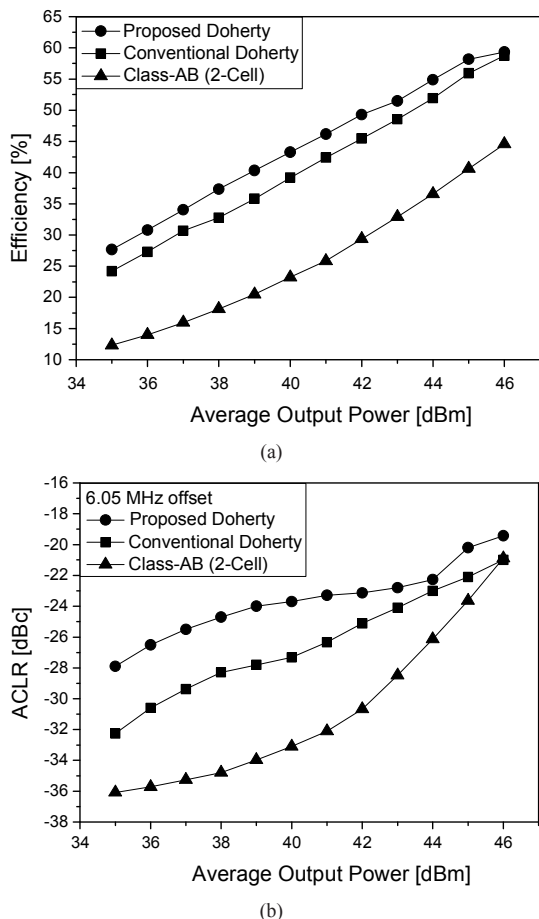


Fig. 14. Measured performances of the conventional and proposed Doherty amplifiers for a WiMAX signal: (a) Drain efficiency. (b) ACLR.

#### A. CW and WiMAX Tests of the Doherty Amplifiers

Fig. 13 shows the measured power characteristics, drain dc currents, and drain efficiencies of the conventional and proposed Doherty PAs for a CW signal. In the experiments, the turn-on power level of the peaking PA is adjusted only by the gate-source voltage  $V_{gs}$ . When the peaking PA is turned off, the load impedance of the proposed carrier PA is higher than that of the conventional PA. Thus, the dc current level of the proposed PA is lower than that of the conventional PA, which leads to improved efficiency at the low power region. However, the peak power of the Doherty PA is degraded because the imperfect load impedance causes an impedance mismatch for  $R_{opt}$  at the peak power region. Although the peak power of the proposed Doherty PA is slightly degraded, the efficiency is increased over a broad output power range.

Fig. 14(a) shows the measured efficiencies for a mobile WiMAX signal with a 10 MHz signal bandwidth and a 7.8 dB PAPR. Compared to the conventional Doherty PA, the efficiency of the proposed PA is improved over a broad average output power level. Fig. 14(b) represents the measured ACLR of the implemented PAs. Because the proposed Doherty PA has a larger load impedance than that of the conventional PA at the low power region and cannot achieve perfect load modulation

TABLE II  
MEASURED PERFORMANCE AT THE 8 dB BACK-OFF OUTPUT POWER FOR A CONVENTIONAL DOHERTY PA AND THE 8 dB AND 7.5 dB BACK-OFF OUTPUT POWERS FOR THE PROPOSED DOHERTY PA

	Conventional Doherty	Proposed Doherty	
$P_{avg}$ [dBm]	42	41.5	42
Back-off level [dB]	8	8	7.5
$\eta_{avg}$ [%]	45.5	48.0	49.3
ACLR [dBc]	-25.1	-23.2	-23.1

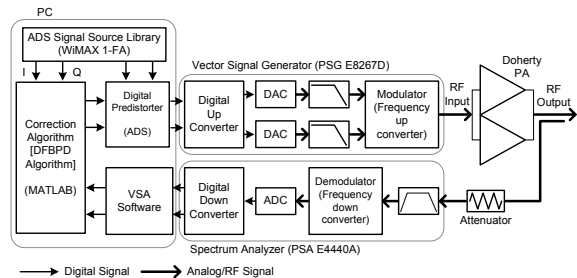


Fig. 15. Experimental setup for linearization.

at the high power region, the ACLR is slightly degraded over the power range. The Doherty PAs also have a worse ACLR than that of the class-AB PA because the peaking PAs are biased at deep class-C to turn off the PAs until the carrier PA is fully saturated, and are optimized to improve the efficiency rather than linearity. In Table II, we summarize the measured efficiencies and ACLRs at the 8 dB back-off output power for a conventional Doherty PA and the 8 dB and 7.5 dB back-off output powers for the proposed Doherty PA. These results allow us to conclude that the proposed Doherty PA has an excellent efficiency with acceptable linearity.

#### B. Linearization Performance of the Amplifier

To confirm the suitability of the proposed Doherty amplifier as the main PA of a base-station or repeater linear power amplifier (LPA) system, we applied the DFBPD linearization technique to the proposed Doherty amplifier. Two 1024-entry AM/AM and AM/PM lookup tables are accomplished by MATLAB program using the DFBPD algorithm as shown in Fig. 15 [24]. The measured spectra before and after compensation for the memoryless nonlinearity by the DFBPD technique are described in Fig. 16. After linearization, the ACLR at an offset of 6.05 MHz is -43 dBc, which is an improvement of approximately 18 dB at an average output

TABLE III  
MEASURED LINEARIZATION PERFORMANCE OF THE PROPOSED DOHERTY AMPLIFIER AT AN AVERAGE OUTPUT POWER OF 42 dBm FOR WiMAX 1FA SIGNAL

	+ / - 5.32 MHz [dBc]	+ / - 6.05 MHz [dBc]	RCE [dB]
<b>Before linearization</b>	-23.5 / -21.8	-25.4 / -23.2	17.7
<b>After linearization</b>	-42.5 / -42.2	-43.0 / -43.0	34.5

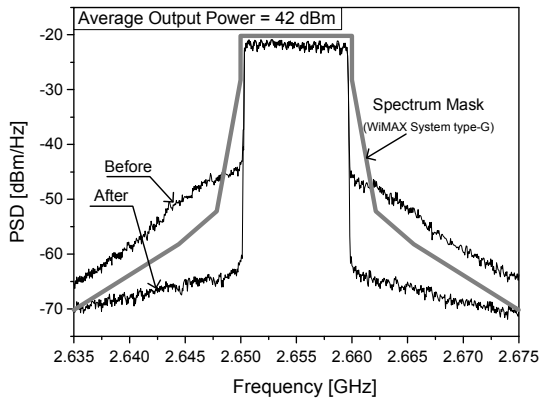


Fig. 16. Measured WiMAX spectra before and after the DFBPD linearization of the Doherty PA at an average output power of 42 dBm.

power of 42 dBm. This spectra satisfies the spectrum mask of the mobile WiMAX system, especially the WiMAX system type-G, (see Fig. 16). The measured signal constellation diagrams before and after the linearization are described in Fig. 17. By linearizing with DFBPD, the relative constellation error (RCE) is  $-34.5$  dB, which is an improvement of about 16.8 dB. These results clearly indicate that after employing the linearization technique, the proposed saturated PA is well suited as a highly efficient main PA of the LPA for the modulated signal. The measured linearization performances are summarized in Table III.

## V. CONCLUSION

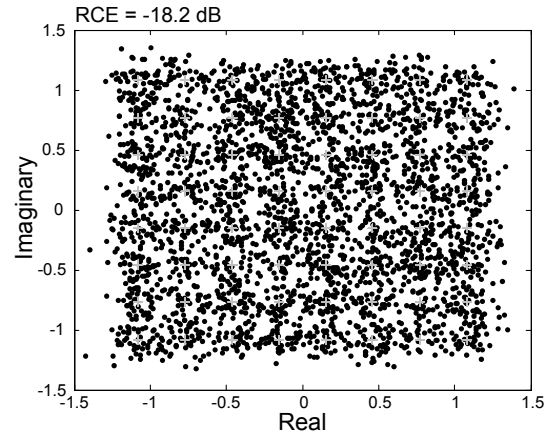
We have investigated the knee voltage effect on the operation of the Doherty PA, especially the carrier PA, to improve efficiency for amplification of modulated signals. From the exploration, we have found that the efficiency at the back-off region of a Doherty PA with  $2R_{opt}$  for the carrier PA is lower than the expected value. To overcome this problem, the carrier PA should employ the load impedance larger than  $2R_{opt}$ . The modified Doherty PA delivers the maximum efficiency at the 6 dB back-off region because the PA is saturated enough at this level while the conventional PA is not. Therefore, the proposed PA delivers better efficiency for the modulated signals. To experimentally validate the amplifier, we have implemented and tested the Doherty PAs using Cree GaN HEMT CGH40045 devices at 2.655 GHz. The experimental results clearly show that the proposed Doherty PA delivers better efficiency at the back-off output power level than the conventional PA with satisfactory linearity because of its better load modulation behavior. The linearity performance is further improved by adopting the DFBPD linearization technique.

## ACKNOWLEDGEMENT

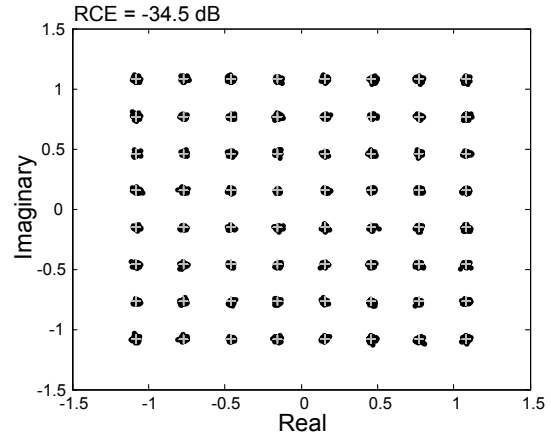
The authors would like to thank to Cree Inc. for providing the GaN HEMT transistors used in this work.

## REFERENCES

[1] F. H. Raab, P. Asbeck, S. Cripps, P. B. Kenington, Z. B. Popović, N. Potheary, J. F. Sevic, and N. O. Sokal, "Power amplifiers and transmitters for RF and microwave," *IEEE Trans. Microw. Theory Tech.*, vol. 50, no. 3, pp. 814–826, Mar. 2002.



(a)



(b)

Fig. 17. Measured WiMAX signal constellation diagram of the Doherty PA at an average output power of 42 dBm: (a) Before linearization. (b) After linearization.

[2] J. Choi, D. Kang, D. Kim, J. Park, B. Jin, and B. Kim, "Power amplifiers and transmitters for next generation mobile handset," *J. Semicond. Technol. Sci.*, vol. 9, no. 4, pp. 249–256, Dec. 2009.

[3] L. Kahn, "Single-sideband transmission by envelope elimination and restoration," *Proc. IRE*, pp. 803–806, Jul. 1952.

[4] D. F. Kimball, J. Jeong, C. Hsia, P. Draxler, S. Lanfranco, W. Nagy, K. Linthicum, L. E. Larson, and P. M. Asbeck, "High-efficiency envelope-tracking W-CDMA base-station amplifier using GaN HFETs," *IEEE Trans. Microw. Theory Tech.*, vol. 54, no. 11, pp. 3848–3856, Nov. 2006.

[5] F. Wang, D. F. Kimball, J. D. Popp, A. H. Yang, D. Y. C. Lie, P. M. Asbeck, and L. E. Larson, "An improved power-added efficiency 19-dBm hybrid envelope elimination and restoration power amplifier for 802.11g WLAN applications," *IEEE Trans. Microw. Theory Tech.*, vol. 54, no. 12, pp. 4086–4099, Dec. 2006.

[6] F. Wang, A. H. Yang, D. F. Kimball, L. E. Larson, and P. M. Asbeck, "Design of wide-bandwidth envelope tracking power amplifiers for OFDM applications," *IEEE Trans. Microw. Theory Tech.*, vol. 53, no. 4, pp. 1244–1255, Apr. 2005.

[7] I. Kim, Y. Y. Woo, J. Kim, J. Moon, J. Kim, and B. Kim, "High-efficiency hybrid EER transmitter using optimized power amplifier," *IEEE Trans. Microw. Theory Tech.*, vol. 56, no. 11, pp. 2582–2593, Nov. 2008.

[8] S.C. Cripps, *RF Power Amplifiers for Wireless Communications*. 2nd ed. Norwood, MA: Artech House, 2006.

[9] W. H. Doherty, "A new high efficiency power amplifier for modulated waves," *Proc. IRE*, vol. 24, no. 9, pp. 1163–1182, Sep. 1936.

[10] F. H. Raab, "Efficiency of Doherty RF power-amplifier systems," *IEEE Trans. Broadcast.*, vol. BC-33, no. 3, pp. 77–83, Sep. 1987.

[11] Y. Yang, J. Yi, Y. Y. Woo, and B. Kim, "Optimum design for linearity and

efficiency of microwave Doherty amplifier using a new load matching technique," *Microw. J.*, vol. 44, no. 12, pp. 20–36, Dec. 2001.

- [12] J. Kim, J. Cha, I. Kim, and B. Kim, "Optimum operation of asymmetrical-cells-based linear Doherty power amplifiers – uneven power drive and power matching," *IEEE Trans. Microw. Theory Tech.*, vol. 53, no. 5, pp. 1802–1809, May 2005.
- [13] Y. Yang, J. Cha, B. Shin, and B. Kim, "A fully matched N-way Doherty amplifier with optimized linearity," *IEEE Trans. Microw. Theory Tech.*, vol. 51, no. 3, pp. 986–993, Mar. 2003.
- [14] M. Iwamoto, A. Williams, P. F. Chen, A. G. Metzger, L. E. Larson, and P. M. Asbeck, "An extended Doherty amplifier with high efficiency over a wide power range," *IEEE Trans. Microw. Theory Tech.*, vol. 49, no. 12, pp. 2472–2479, Dec. 2001.
- [15] N. Srirattana, A. Raghavan, D. Heo, P. E. Allen, and J. Laskar, "Analysis and design of a high-efficiency multistage Doherty power amplifier for wireless communications," *IEEE Trans. Microw. Theory Tech.*, vol. 53, no. 3, pp. 852–860, Mar. 2003.
- [16] J. Moon, J. Kim, I. Kim, J. Kim, and B. Kim, "Highly efficient three-way saturated Doherty amplifier with digital feedback predistortion," *IEEE Microw. Wireless Compon. Lett.*, vol. 18, no. 8, pp. 539–541, Aug. 2008.
- [17] J. Kim, J. Moon, Y. Y. Woo, S. Hong, I. Kim, J. Kim, and B. Kim, "Analysis of a fully matched saturated Doherty amplifier with excellent efficiency," *IEEE Trans. Microw. Theory Tech.*, vol. 56, no. 2, pp. 328–338, Feb. 2008.
- [18] S. Goto, T. Kuni, A. Inoue, K. Izawa, T. Ishikawa, and Y. Matsuda, "Efficiency enhancement of Doherty amplifier with combination of class-F and inverse class-F schemes for S-band base station application," in *IEEE MTT-S Int. Microw. symp. Dig.*, Jun. 2004, pp. 839–842.
- [19] Y. Suzuki, T. Hirota, and T. Nojima, "Highly efficient feed-forward amplifier using a class-F Doherty amplifier," in *IEEE MTT-S Int. Microw. symp. Dig.*, Jun. 2003, pp. 77–80.
- [20] J. Moon, Y. Y. Woo, and B. Kim, "A highly efficient Doherty power amplifier employing optimized carrier cell," in *Proc. 39th Eur. Microw. Conf.*, Sep. 28–Oct. 2 2009, pp. 1720–1723.
- [21] K. Horiguchi, S. Ishizaka, T. Okano, M. Nakayama, H. Ryoji, Y. Isota, and T. Takagi, "Efficiency enhancement of 250 W Doherty power amplifier using virtual open stub techniques for UHF-band OFDM applications," in *IEEE MTT-S Int. Microw. symp. Dig.*, Jun. 2006, pp. 1356–1359.
- [22] N. Ui, H. Sano, and S. Sano, "A 80 W 2-stage GaN HEMT Doherty amplifier with –50 dBc ACLR, 40% efficiency, 32 dB gain with DPD for W-CDMA base station," in *IEEE MTT-S Int. Microw. symp. Dig.*, Jun. 2007, pp. 1259–1262.
- [23] R. Sweeney, "Practical magic," *IEEE Microw. Mag.*, vol. 9, no. 2, pp. 73–82, Apr. 2008.
- [24] Y. Y. Woo, J. Kim, J. Yi, S. Hong, I. Kim, J. Moon, and B. Kim, "Adaptive digital feedback predistortion technique for linearizing power amplifier," *IEEE Trans. Microw. Theory Tech.*, vol. 55, no. 5, pp. 932–940, May 2007.



**Junghwan Moon** (S'07) received the B.S. degree in electrical and computer engineering from the University of Seoul, Seoul, Korea, in 2006 and is currently working toward the Ph.D. degree at the Pohang University of Science and Technology (POSTECH), Pohang, Gyungbuk, Korea.

His current research interests include highly linear and efficient RF PA design, memory-effect compensation techniques, digital predistortion (DPD) techniques, and wideband RF PA design.

Mr. Moon was the recipient of the Highest Efficiency Award at Student High-Efficiency Power Amplifier Design Competition in IEEE MTT-S International Microwave Symposium (IMS), 2008.



**Jangheon Kim** (S'07-M'09) received the B.S. degree in electronics and information engineering from Chon-buk National University, Chonju, Korea, in 2003, and the Ph.D. degree in electrical engineering from the Pohang University of Science and Technology (POSTECH), Pohang, Gyungbuk, Korea, in 2009.

He is currently a senior engineer with the Network Division, Digital Media & Communications, Samsung Electronics Company Ltd., Suwon, Republic of Korea. From 2009 to 2010, he was a post-doctoral

Fellow with the University of Waterloo, Waterloo, ON, Canada. His current research interests include highly linear and efficient RF PA design, digital predistortion (DPD) techniques, and highly efficient transmitter for wireless communication systems.

Dr. Kim was the recipient of the Highest Efficiency Award at Student High-Efficiency Power Amplifier Design Competition in IEEE MTT-S International Microwave Symposium (IMS), 2008, and 2010 MICROWAVE AND WIRELESS COMPONENTS LETTERS Outstanding Reviewer Award, 2010.



**Jungjoon Kim** received the B.S. degree in electrical engineering from Han-Yang University, Ansan, Korea, in 2007, and the Master degree in electrical engineering from the Pohang University of Science and Technology (POSTECH), Pohang, Gyungbuk, Korea, in 2009. He is currently working toward the Ph.D. degree at the POSTECH, Pohang, Gyungbuk, Korea.

His current research interests include RF PA design and supply modulator design for highly efficient transmitter system.



**Ildu Kim** received his B.S. degree in electronics and information engineering from Chon-nam National University, Kwangju, Korea, in 2004 and the Ph.D. degree in Pohang University of Science and Technology (POSTECH), Pohang, Korea, in 2010. In 2010, he joined the Samsung Electronics Company Ltd., Suwon, Gyeonggi, Korea.

His current research interests include highly linear and efficient RF power amplifier design, linear power amplifier (LPA) system design and highly linear and efficient RF transmitter architectures.



**Bumman Kim** (M'78-SM'97-F'07) received the Ph.D. degree in electrical engineering from Carnegie Mellon University, Pittsburgh, PA, in 1979.

From 1978 to 1981, he was engaged in fiber-optic network component research with GTE Laboratories Inc. In 1981, he joined the Central Research Laboratories, Texas Instruments Incorporated, where he was involved in development of GaAs power field-effect transistors (FETs) and monolithic microwave integrated circuits (MMICs). He has developed a large-signal model of a power FET, dual-gate FETs

for gain control, high-power distributed amplifiers, and various millimeter-wave MMICs. In 1989, he joined the Pohang University of Science and Technology (POSTECH), Pohang, Gyungbuk, Korea, where he is a POSTECH Fellow and a Namko Professor with the Department of Electrical Engineering, and Director of the Microwave Application Research Center, where he is involved in device and circuit technology for RF integrated circuits (RFICs). He has authored over 300 technical papers.

Prof. Kim is a member of the Korean Academy of Science and Technology and the National Academy of Engineering of Korea. He was an associate editor for the IEEE TRANSACTIONS ON MICROWAVE THEORY AND TECHNIQUES, a Distinguished Lecturer of the IEEE Microwave Theory and Techniques Society (IEEE MTT-S), and an AdCom member.